

Small Signal Stability Assessment of MEPE Test System in Free and Open Source Software

Kyaw Myo Lin

Abstract—This paper presents small signal stability study carried over the 140-Bus, 31-Machine, 5-Area MEPE system and validated on free and open source software: PSAT. Well-established linear-algebra analysis, eigenvalue analysis, is employed to determine the small signal dynamic behavior of test system. The aspects of local and interarea oscillations which may affect the operation and behavior of power system are analyzed. Eigenvalue analysis is carried out to investigate the small signal behavior of test system and the participation factors have been determined to identify the participation of the states in the variation of different mode shapes. Also, the variations in oscillatory modes are presented to observe the damping performance of the test system.

Keywords—Eigenvalue analysis, Mode shapes, MEPE test system, Participation factors, Power System oscillations.

I. INTRODUCTION

TWO of the most important design criteria for multi-machine power systems are transient stability and damping of electromechanical modes of sustained oscillation [1]-[6]. Stability of power systems is one of the most important aspects in power electrical operation. This is because power system must maintain frequency and voltage levels in the desired level, under any disturbance [7]. With the increase of the scale and complexity of the interconnected power networks, the problems on the various potential power oscillations, which have the significance impact on the system stability and security operation, have been drawn more and more attention [8]-[10].

The small signal dynamic behavior of power systems can be determined by eigenvalue analysis, which is a well-established linear-algebra analysis method [11], if a dynamic power system model is available. In an analysis of the system stability, eigenvalues of a power system model have been derived and evaluated. Through analyzing eigenvalues, characteristics of system dynamic states are understood without a time domain simulation. Hence, the eigenvalue analysis is efficient in appraising the system stability for a multi-machine power system model. The system eigenvalues have been evaluated with respect to the components of the power grid; that is to say, the eigenvalues with regard to electrical distances between generators.

Mr. Kyaw Myo Lin is a PhD research candidate with the Power System Research Unit at the Department of Electrical Power Engineering, Mandalay Technological University, Patheingyi, Mandalay Region, Myanmar (Phone: (95-9) 256126590; (95-2) 57360 Fax: (95-2) 88702; e-mail: kmlp2381@gmail.com, linkyawmyo@yahoo.com).

In the large power systems, small signal stability problems may be either local or global (interarea) in nature. Local problems involve a small part of the system. They may be associated with rotor angle oscillations of single generator or a single plant against the rest of the power system. Such oscillations are called local plant mode oscillations [12]. Local problems may also be associated with oscillations between the rotors of a few generators close to each other. Such oscillations are called inter-machine or interplant mode oscillations [12]. Global small signal stability problems are caused by interactions among large groups of generators and have widespread effects. They involve oscillations of a group of generators in one area swinging against a group of generators in another area. Such oscillations are called interarea mode oscillations [9].

In this paper, real case off-line system namely Myanmar national grid test system (MEPE test system) is applied and tested. The MEPE electricity network is largely supplied by hydro power while supplying large consumption in the Yangon area and central region through weak transmission lines [13]. Hydro power in Myanmar accounts for more than three-quarter (about 76 percents) of net production of electrical generation. In hydro power production systems, the functions of hydro turbine and governors cannot be neglected because they participate in primary frequency control of power systems [14]. Features of hydro generators are substantially different from those of thermal generators, and their respective modeling needs to be done appropriately [15].

Power System Analysis Toolbox (PSAT[®]) [16], an educational free and open source (FOSS) for power system analysis studies [17] is employed as a simulation tool in this study. The toolbox covers fundamental and necessary routines for power system studies such as power flow, small signal stability analysis and time domain simulation. PSAT is a suitable candidate as power system analysis software which is capable of performing core stability analyses.

The aim of this paper is to propose an improved model of the modified MEPE power system in FOSS for power system stability analyses and studies. The study model includes a newly developed hydro turbine and hydro governor model [15] which is capable of representing the actual dynamic behavior of hydro units. The paper is organized in five sections. The small signal stability and eigenvalue analysis has been discussed in Section II. Section III details the test system characteristics and dynamic modeling. Simulation and results with two different scenarios are presented and discussed in Section IV followed by the conclusion in Section V.

II. SMALL SIGNAL STABILITY

The small signal stability, and more broadly the dynamic performance, of the power system are related to the damping of the electromechanical modes of oscillation. This oscillatory behavior is associated fundamentally with (i) the variation in the electrical torque developed by synchronous machines as their rotor angles change; and (ii) the inertia of their rotors. The frequencies associated with these modes of oscillation are typically in the range from 0.5 to 4 Hz.

A. Modes of Oscillation

The analysis of small signal stability is particularly of interest of electromechanical modes of oscillations. It involves the rotors of individual generators or groups of generators oscillating or swinging against each other. Electromechanical modes of oscillation can be broadly subdivided into (i) local area modes having frequency range of 0.7–2 Hz and (ii) inter-area modes having frequency range of 0.16–0.7 Hz [8, 18]. Small signal stability requires that these modes should be adequately damped. The presence of AVR and PSS greatly influences the damping of these modes and can be assessed by means of eigenvalue analysis.

The eigenvalue analysis can be carried out by linearizing the system about an operating point and representing it in state space form. For stability, all of the eigenvalues must lie in the left half complex plane. Any eigenvalue in the right half plane denotes an unstable dynamic mode and system instability. The damping contribution provided by any means shifts the location of the eigenvalues associated with the dominant oscillatory modes to the left half of the plane.

B. Eigenvalue Computation

The behavior of a dynamic system, such a power system, can be described by the complete set of n-first order non-linear ordinary differential and algebraic equations (DAE) of the following form [8], [19].

$$\begin{aligned} \dot{x} &= f(x, z, u) \\ 0 &= g(x, z, u) \end{aligned} \quad (1)$$

where, x takes the values of 1 to n; n is the order of the system.

At the equilibrium, all time derivatives of the states are zero and are obtained from a load flow analysis.

$$\begin{aligned} 0 &= f(x_0, z_0, u_0) \\ 0 &= g(x_0, z_0, u_0) \end{aligned} \quad (2)$$

The complete set of differential equations with network equations are arranged in state-space form and linearized about an operating point as;

$$[\Delta \dot{x}] = [A][\Delta x] + [B][\Delta z] \quad (3)$$

In the small signal perturbed model:

$$\begin{aligned} [\Delta x] &= [\Delta \delta, \Delta \omega, \Delta E]^T \\ [\Delta z] &= [\Delta \theta_1, \Delta \theta_2, \Delta \theta_3, \Delta V_1, \Delta V_2, \Delta V_3]^T \end{aligned} \quad (4)$$

By taking the Laplace transform of above equations

$$\Delta x(s) = \frac{adj(sI - A)}{\det(sI - A)} [\Delta x(0) + B\Delta u(s)] \quad (5)$$

Similarly,

$$\Delta z(s) = \frac{adj(sI - A)}{\det(sI - A)} [\Delta z(0) + B\Delta u(s) + D\Delta u(s)] \quad (6)$$

The poles of the system are the roots of the characteristic equations given by

$$\det(sI - A) = 0 \quad (7)$$

Above equation can be written as characteristic equation

$$\det(A - \lambda I) = 0 \quad (8)$$

The values of λ ($\lambda = \lambda_1, \lambda_2, \lambda_3 \dots \lambda_n$) which satisfy the characteristic equation, are known as the eigenvalues of matrix A. The numbers of eigenvalues are equal to the number of first-order differential equations considered in the model to represent the system. Eigenvalues may be real or complex, if the matrix is real.

The complex eigenvalues always occur in conjugate pairs, as shown;

$$\lambda_i = \alpha_i \pm j\beta_i \quad (9)$$

For a given eigenvalue, damping ratio, frequency oscillation, and time constant can be calculated using the following expressions;

$$\zeta = \frac{-\alpha}{\sqrt{\alpha^2 + \beta^2}}, f = \frac{\beta}{2\pi}, t = \frac{1}{\alpha} \quad (10)$$

In this work, eigenvalues have been calculated along with damping ratio and frequency of oscillation for different cases and the participation factor of mode i, can be computed as follows;

$$p_i = \begin{pmatrix} p_{1i} \\ p_{2i} \\ \dots \\ p_{mi} \end{pmatrix} \quad (11)$$

$$p_{ki} = \frac{|\Phi_{ki}| |\Psi_{ki}|}{\sum_{k=1}^n |\Phi_{ki}| |\Psi_{ki}|} \quad (12)$$

where, m is the number of state variables, p_{ki} is the participation factor of the kth state variable into mode i, Φ_{ki} is the ith element of the kth right eigenvector of A, Ψ_{ki} is the mth element of the ith left eigenvector of A.

III. MEPE TEST SYSTEM

A. Background

Myanmar has an installed capacity of approximately 3,460 MW of energy generation, which is composed primarily of 2,660 MW (about 76%) of hydro capacity, 550 MW (about 16%) of gas-fired capacity, 165 MW (about 5%) steam capacity and 120 MW (3.5%) of coal-fired capacity [20, 21].

Currently, the total installed capacity of the hydropower plants is 2,660 MW with a firm capacity of 1,504 MW, out of which 860 MW is in reservoir-based plants and the rest in run-of-river plants. Hydropower accounts for about 76 percent of installed capacity and 65 percent of electricity production. The system analyzed in this study is a conceptualization of MEPE grid circa 2014. It is based on a system data proposed by KEPCO (consultant of MEPE) and the staffs of power system department of MEPE.

B. System Characteristics

The MEPE system is depicted in Fig. 1. The voltage levels of the test system are 230 kV, 132kV, 66kV and 33kV respectively. The grid study is valid for the transmission system only and do not include the distribution network. The grid has no direct connections to other grids of neighboring countries.

The five areas of MEPE test system are:

- “West” with two hydro generating stations and four thermal generations and some loads,
- “North” with only four hydro generations and some loads,
- “East” with only one coal-fired station and five hydro stations and some loads,
- “Central” with much loads and eight hydro generating stations, and
- “YESB” with heavy loads and seven thermal generating stations.

C. Dynamic Modeling

Dynamic models of synchronous generators, exciters, turbines, and governors for MEPE power system are implemented in PSAT. All models used are documented in the PSAT manual.

1) Generator Models

Two synchronous machine models are used in the system: three-rotor windings for the salient-pole machines of hydro power plants and four-rotor windings for the round-rotor machines of thermal plants. These two types of generators are described by five and six state variables, respectively: δ , ω , e'_q , e''_q and e''_d and with an additional state e'_d for the six state variable machines. All generators have no mechanical damping and saturation effects are neglected. In the test system (Fig.1), the generating stations namely: G1, G2, G3, G4, G5, G6, G7, G8, G9, G10, G12, G13 and G21 are the thermal generating stations and the rest are the hydro generating units.

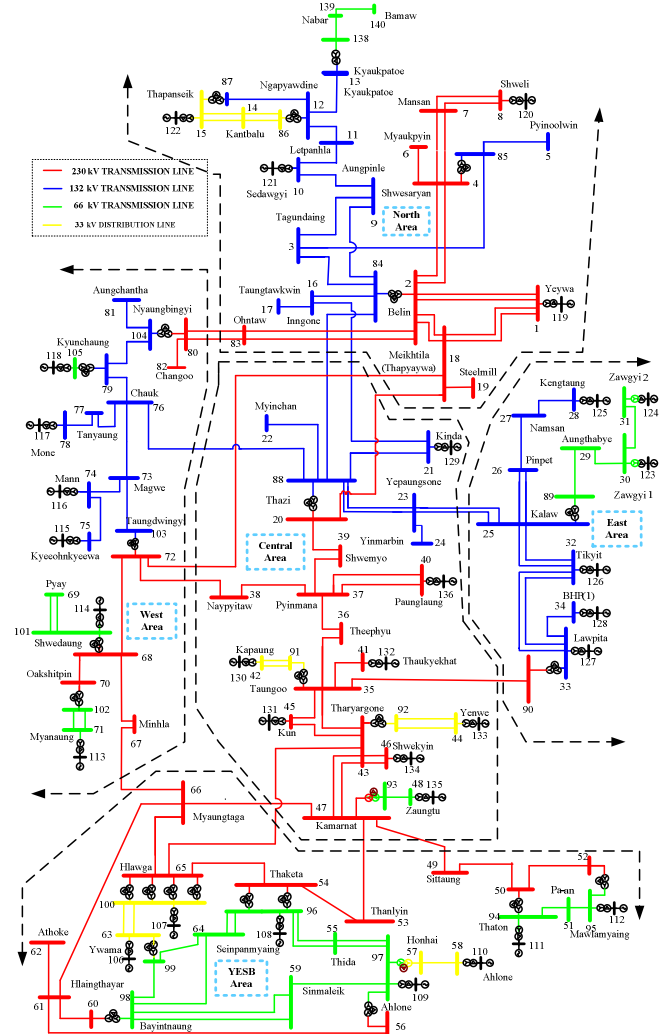


Fig. 1 MEPE test system

2) Automatic Voltage Regulator Models:

The same model of AVR, as shown in Fig. 2, is used for all generators but with different parameters. The field voltage v_f is subject to an anti-windup limiter.

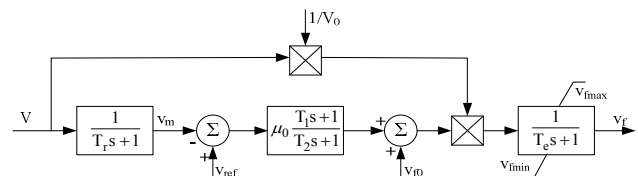


Fig. 2 Exciter model

3) Turbine and Governor Models

In PSAT, there are three models of turbine and governors: namely Model 1, Model 2 and Model 3. The first one is a thermal generator model while the second is a simplified model. As such, the system's hydro generator is temporarily represented by Model 2 while that of thermal is represented by Model 1. Block diagrams of these two models are depicted in Figs. 3 and 4, respectively.

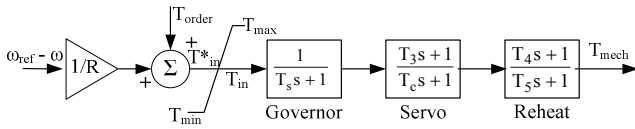


Fig. 3 Turbine governor model used for thermal generator: Model 1

W. Li et al. recently developed hydro turbine and governor models in PSAT [14]. The block diagram of Model 3 is shown in Fig. 5.

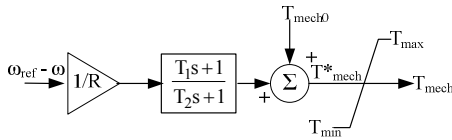


Fig. 4 Turbine governor model used for simple hydro generator: Model 2

Hydro turbine and governor are normally combined together for representation. The block consists of a typical hydro turbine governor and a linearized hydro turbine model where the corresponding elements are depicted in the figure. The linearized turbine is the classical hydro turbine model in power system stability analysis, corresponding to ideal turbine and inelastic penstock with water inertial effect considered.

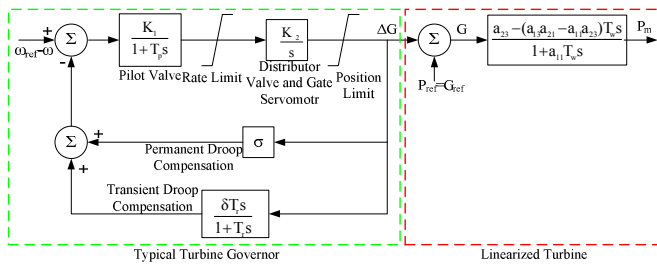


Fig. 5 Turbine and governor model used for typical hydro generator: Model 3

IV. RESULTS AND DISCUSSION

Small signal stability analysis reveals important relationships among state variables of a system and gives an insight into the electromechanical dynamics of the network. Applying the well-established linear-algebra analysis technique to the linearized model of the MEPE test system, small signal stability is studied by analyzing four properties: eigenvalues, frequencies of oscillation, damping ratios and eigenvectors (or mode shapes). Fig. 6 depicts the user interface for small signal stability analysis.

Before fulfilling eigenvalue analysis, it is necessary to calculate power flow. After solving the power flow problem, it is possible to compute and visualize the eigenvalues and the participation factors of the system. For this reason, power flow calculation has been carried out. In PSAT, there are seven power flow solvers already implemented. In this analysis, 4th order Runge-Kutta solver is applied for its high accuracy rate of state variable initialization. To conduct a load flow study,

bus number 119 (Yeywa Hydro Power Station Bus) is selected as the slack bus and other generating buses have been used as voltage controlled bus. The results of power flow are not shown here because it is just only the state variable initializations for small signal stability analysis.

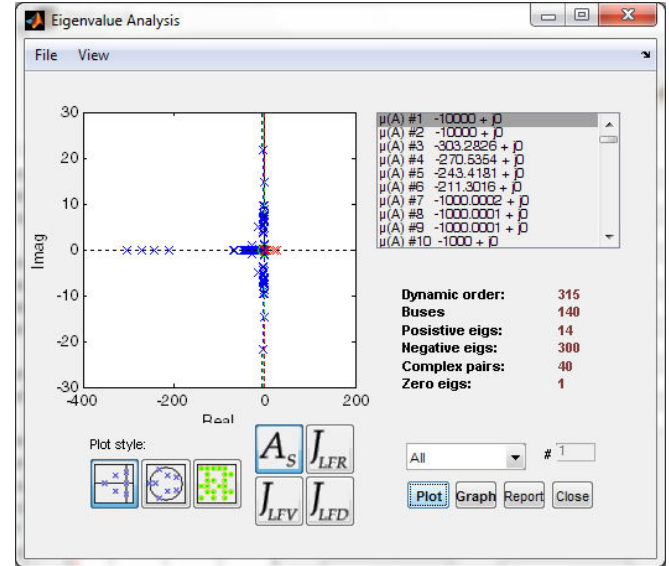


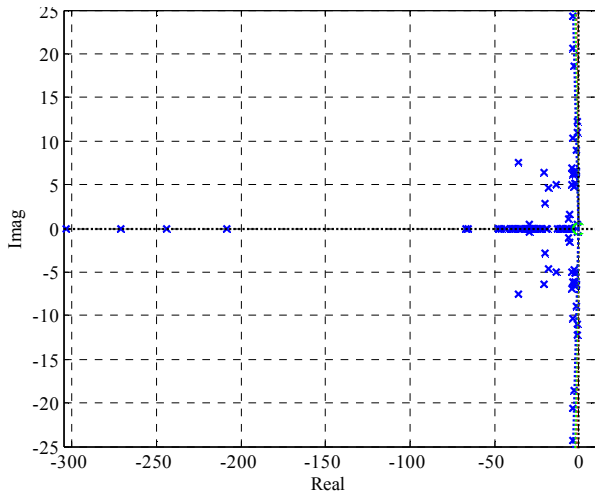
Fig. 6 GUI for small signal stability analysis

Several options are available for adjusting the performance and the changing the output of the routine. It is possible to set the output map, the Jacobian matrix and the number and kind of eigenvalues to be computed.

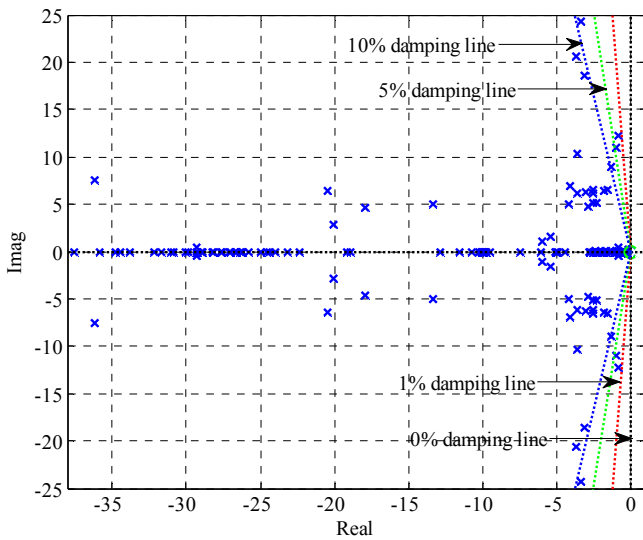
A. Eigenvalue Analysis of Test System

For linear analysis of test system, the benchmark system is implemented with Model 1 and Model 2 as well as Model 1 and Model 3. The system has 315 states with Model 2 while 372 states with Model 3; the number corresponds to the same number of eigenvalues. Plot of eigenvalues of test system implementing Model 2 and Model 3 are illustrated in Figs. 7 and 8, showing their respective local enlargement.

The small signal stability analysis has been carried out for the benchmark system and all eigenvalues for the MEPE benchmark system, either with Model 2 or Model 3, are located in the left half plane, which indicates systems are stable. From the figures above, all eigenvalues have negative real part so that the system is said to be inherently dynamically stable. Comparing the figures, it can be observed that there are more eigenvalues having lower damping ratios in the system with Model 3 than that with Model 2. For the system with Model 2, there are six paired complex eigenvalues located outside the 10% damping line. For the system with Model 3, there are twelve paired complex eigenvalues located outside the 10% damping line because of Model 2 doesn't compose of nonlinear dynamic and only represents simple and classical model.



(a) Model 2

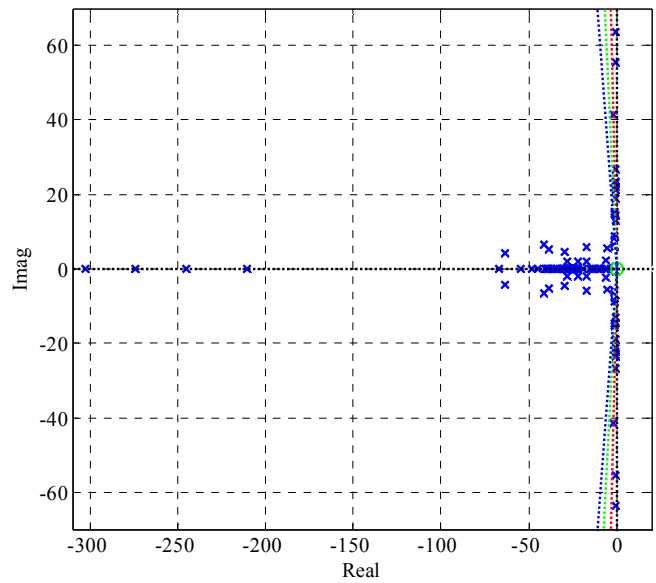


(b) Model 2 (Local enlargement)

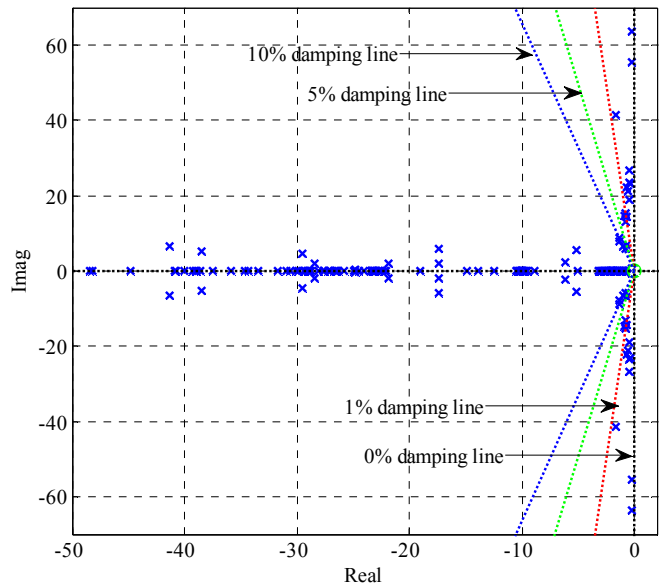
Fig. 7 Eigenvalues of the MEPE test system with Model 2

Table I provides the two lowest damping modes, their corresponding frequencies and damping ratios and the most associated state variables for both scenarios considering the case with Model 2 and the case with Model 3. As shown in the following table, the damping ratios obtained from the two models bear a significance difference. This discrepancy is due to the incorrect modeling of the hydro turbine and governor using Model 2, from which damping ratios are larger than when using Model 3 for hydro turbine and governor representation.

This model error might influence the design of damping controllers to be less effective; this precisely illustrate why hydro turbine and governor modeling is important.



(a) Model 3



(b) Model 3 (Local enlargement)

Fig. 8 Eigenvalues of the MEPE test system with Model 3

TABLE I
 LINEAR ANALYSIS RESULTS OF THE TWO LOWEST DAMPING MODES

Model	Eigenvalues	Frequency (Hz)	Damping Ratio	Most Associated States
Model 2	$-0.01752 \pm j1.6582$	0.26391	0.01057	δ_{14}, ω_{14}
	$-0.05496 \pm j4.1796$	0.665204	0.01315	ω_8, δ_8
Model 3	$-0.003686 \pm j2.4261$	0.38613	0.001519	ω_{14}, δ_{14}
	$-0.005229 \pm j3.6698$	0.58407	0.001425	ω_2, δ_2

B. Electromechanical and Interarea Modes of Test System

Local modes or machine-system modes relate to the swinging of generators with respect to the rest of the power system. Interarea modes relate to the groups of machines from different parts that swing against each other. This problem

occurs because of weak tie-line interconnection. It was observed that all the poorly damped (i.e. damping ratio less than 10%) or unstable modes had high participation from rotor angles and rotor speed of various machines.

In this research, the participation factor has been utilized to determine the dominant generator because the load angle of a generator that has the highest participation factor on the main dominant interarea modes, affects the power system stability. Participation factors for both cases of the MEPE test system are shown in Figs. 9 and 10, respectively.

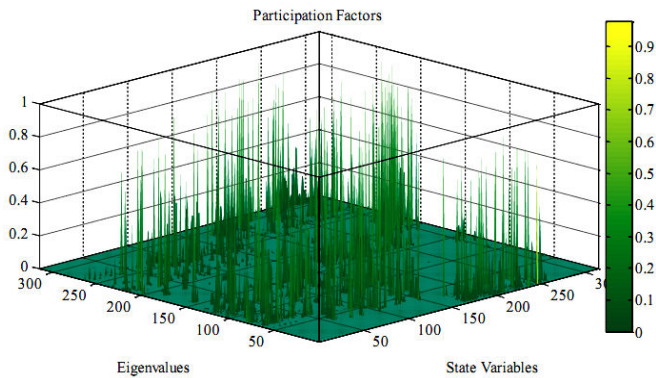


Fig. 9 System Participation Factors in Test System for all Eigenvalues and State Variables (Model 1 & Model 2)

As discussed in previous section, the system has 315 eigenvalues with Model 2 and 372 eigenvalues with Model 3. The presence of Model 3 changes the system states from 315 to 372. There are 39 complex pairs among those eigenvalues for the test system with Model 2 and 40 complex pairs for Model 3.

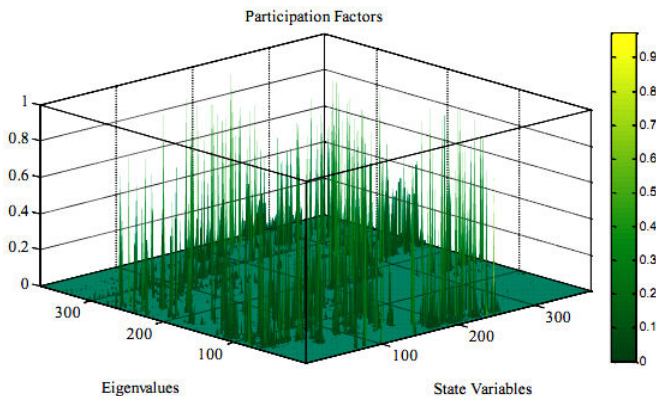


Fig. 10 System Participation Factors in Test System for all Eigenvalues and State Variables (Model 1 & Model 3)

These complex pairs were observed as critical mode. However, for the scope of the study, only two criteria: 0.4~0.7Hz and 0.7~2Hz are observed. The particular network oscillatory response characteristics giving the frequency of oscillations, damping ratio and three most influencing states with their participation of two cases are denoted in Tables II and III, respectively.

In these two tables, the participation factors most associated with the eigenvalues are listed and the relation between the modes, state variables (especially generator angles and speeds) and machines are also shown. For the test system with Model 2, the strong related generators are G14, G9, G8, G18, G7, G31, G20, G1, G27, G22, G23 and G2 while for the system with Model 3, G14, G29, G2, G18, G30, G20, G16, G1, G8, G31, G23, G27 and G13 are notified as the strong related generators. As discussed in previous section, G14 is the lowest damping mode in both cases.

According to the results of these two tables, the strong relative generators with high participation should be considered to determine the optimal location for installing power oscillations dampers (PODs) such as power system stabilizers (PSSs). It is expected that by installing a PSS at the generator having the largest magnitude at the mode of interest, a more significant damping than installing at the other generators.

The system response characteristics are comprised of an amalgam of the dynamic modes identified by system eigenvalues. Hence, it is not possible to directly link specific responses with individual eigenvalues. However, the dominant oscillatory modes of the test system are shown in the tables.

For the case study with Model 2, the particular network oscillatory response characteristics are classified as follows:

- Mode 1 having a frequency of 0.26391 Hz corresponds to the interarea mode between North and West,
- Mode 2 having a frequency of 0.47639 Hz corresponds to the interarea mode between West and YESB,
- Mode 3 having a frequency of 0.665204 Hz corresponds to the interarea mode between West and Central,
- Mode 4 having a frequency of 0.68383 Hz corresponds to the interarea mode between East and Central,
- Mode 5 having a frequency of 0.6997 Hz corresponds to the interarea mode between YESB and Central,
- Mode 6 having a frequency of 0.75892 Hz, mode 10 having a frequency of 1.4018 Hz, and mode 11 having a frequency of 1.4892 Hz correspond to the local modes in Central,
- Mode 7 having a frequency of 0.87292 Hz corresponds to the local mode in North,
- Mode 8 having a frequency of 0.95786 Hz, mode 12 having a frequency of 1.5059 Hz and mode 13 having a frequency of 1.8897 correspond to the local modes in East,
- Mode 9 having a frequency of 1.0714 Hz and Mode 14 having a frequency of 1.9092 Hz corresponds to the local mode in YESB.

For the case study with Model 3, the particular network oscillatory response characteristics are classified as follows:

- Mode 1 having a frequency of 0.38613 Hz corresponds to the interarea mode between North and Central,
- Mode 2 having a frequency of 0.3924 Hz corresponds to the interarea mode between Central and YESB,

- Mode 3 having a frequency of 0.58407 Hz corresponds to the interarea mode between YESB and West,
- Mode 4 having a frequency of 0.62698 Hz corresponds to the interarea mode between East and Central,
- Mode 5 having a frequency of 0.6325 Hz corresponds to the interarea mode between Central and West,
- Mode 6 having a frequency of 0.80853 Hz, mode 11 having a frequency of 1.2207 Hz, mode 13 having a frequency of 1.3056 Hz and mode 15 having a frequency of 1.6232 Hz correspond to the local mode in East,
- Mode 7 having a frequency of 0.85564 Hz corresponds to the local mode in North,
- Mode 8 having a frequency of 0.91724 Hz corresponds to the local mode in YESB,
- Mode 9 having a frequency of 0.93217 Hz and mode 14 having a frequency of 1.4242 Hz correspond to the local modes in West, and
- Mode 10 having a frequency of 0.94624 Hz and mode 12 having a frequency of 1.2032 Hz correspond to the local modes in Central.

TABLE II
 DOMINANT OSCILLATORY MODES OF TEST SYSTEM WITH MODEL 2

Mode No.	Eigenvalues	Frequency (Hz)	Damping Ratio	Most Influence State in the Control of the Mode with their % Participation		
(1)	$\lambda_{125}, \lambda_{126}$	-0.01752±j1.6582	0.26391	0.01057	$\delta_{14} = 42.8\%$ $\omega_{14} = 42.8\%$	$\delta_{13} = 2.8\%$
(2)	$\lambda_{156}, \lambda_{157}$	-6.6165±j2.9929	0.47639	0.9111	$e_{d9} = 13.8\%$ $\omega_9 = 11.8\%$	$\omega_2 = 2.1\%$
(3)	$\lambda_{152}, \lambda_{154}$	-0.05496±j4.1796	0.665204	0.01315	$\omega_8 = 35.2\%$ $\delta_8 = 22.3\%$	$\omega_{27} = 17.1\%$
(4)	$\lambda_{148}, \lambda_{149}$	-5.2158±j4.2966	0.68383	0.7718	$e_{d18} = 19\%$ $\omega_{13} = 18.8\%$	$\omega_6 = 11\%$
(5)	$\lambda_{150}, \lambda_{151}$	-5.4965±j4.3963	0.6997	0.7809	$e_{d7} = 16.8\%$ $\delta_7 = 12.2\%$	$\omega_{27} = 8.6\%$
(6)	$\lambda_{122}, \lambda_{123}$	-18.1788±j4.7741	0.75892	0.9672	$\omega_{31} = 42.8\%$ $\delta_{31} = 42.8\%$	$e_{d31} = 2.8\%$
(7)	$\lambda_{146}, \lambda_{147}$	-4.3436±j5.4847	0.87292	0.6208	$e_{d8} = 11.6\%$ $\delta_{14} = 42.8\%$	$e_{d14} = 2.8\%$
(8)	$\lambda_{143}, \lambda_{144}$	-4.2221±j6.0184	0.95786	0.5741	$\delta_{20} = 14.6\%$ $\omega_{20} = 14.7\%$	$e_{d20} = 7.18\%$
(9)	$\lambda_{135}, \lambda_{136}$	-2.624±j6.7318	1.0714	0.3632	$\omega_1 = 24.9\%$ $\delta_1 = 24.5\%$	$\omega_7 = 9.1\%$
(10)	$\lambda_{132}, \lambda_{133}$	-2.7469±j8.8079	1.4018	0.2977	$\omega_{30} = 23.4\%$ $\delta_{30} = 23.4\%$	$e_{d30} = 2.8\%$
(11)	$\lambda_{130}, \lambda_{131}$	-7.8929±j9.3567	1.4892	0.6448	$\delta_{27} = 19.9\%$ $\omega_{27} = 19\%$	$e_{d27} = 11.8\%$
(12)	$\lambda_{101}, \lambda_{102}$	-9.584±j9.4617	1.5059	0.7116	$\omega_{22} = 30.4\%$ $\delta_{22} = 17.9\%$	$e_{d22} = 7.5\%$
(13)	$\lambda_{118}, \lambda_{119}$	-6.9917±j11.8734	1.8897	0.5074	$\omega_{23} = 18.1\%$ $\delta_{23} = 13.7\%$	$\omega_{10} = 2.11\%$
(14)	$\lambda_{114}, \lambda_{115}$	-2.5869±j11.9957	1.9092	0.2108	$\omega_2 = 18.3\%$ $\delta_2 = 17\%$	$e_{d2} = 5.6\%$

TABLE III
 DOMINANT OSCILLATORY MODES OF TEST SYSTEM WITH MODEL 2

Mode No.	Eigenvalues	Frequency (Hz)	Damping Ratio	Most Influence State in the Control of the Mode with their % Participation		
(1)	$\lambda_{87}, \lambda_{88}$	-0.00369±j2.4261	0.38613	0.00152	$\omega_{14} = 49.1\%$ $\delta_{14} = 22.8\%$	$\delta_{27} = 7.1\%$
(2)	$\lambda_{101}, \lambda_{102}$	-18.8501±j3.4654	0.3924	0.9916	$e_{d29} = 23.4\%$ $\delta_{29} = 23.2\%$	$\delta_2 = 17\%$
(3)	$\lambda_{295}, \lambda_{296}$	-0.00523±j3.6698	0.58407	0.001425	$\omega_2 = 21.1\%$ $\delta_{14} = 42.8\%$	$\omega_{11} = 12\%$
(4)	$\lambda_{176}, \lambda_{177}$	-4.1909±j3.9394	0.62698	0.7286	$e_{d18} = 30.4\%$ $\omega_{18} = 21\%$	$\delta_{26} = 10.1\%$
(5)	$\lambda_{99}, \lambda_{100}$	-22.2064±j3.9739	0.6325	0.9844	$e_{d30} = 48\%$ $\delta_{30} = 42.8\%$	$\omega_{30} = 21\%$
(6)	$\lambda_{176}, \lambda_{177}$	-3.621±j5.0802	0.80853	0.5804	$\omega_{20} = 19.2\%$ $\delta_{20} = 18.9\%$	$e_{d20} = 4.13\%$
(7)	$\lambda_{171}, \lambda_{172}$	-2.3587±j5.3762	0.85564	0.4018	$\omega_{16} = 17.5\%$ $\delta_{16} = 17.5\%$	$e_{q16} = 9.9\%$
(8)	$\lambda_{166}, \lambda_{167}$	-1.9203±j5.7635	0.91729	0.3161	$\omega_1 = 19.2\%$ $\delta_1 = 18.9\%$	$e_{d1} = 4.13\%$
(9)	$\lambda_{161}, \lambda_{162}$	-0.25471±j5.857	0.93217	0.0434	$e_{d8} = 16.5\%$ $e_{q8} = 14\%$	$\omega_8 = 1.13\%$
(10)	$\lambda_{164}, \lambda_{165}$	-1.6388±j5.9454	0.94624	0.2657	$\omega_{31} = 22.3\%$ $\delta_{31} = 18.9\%$	$e_{d31} = 6\%$
(11)	$\lambda_{149}, \lambda_{150}$	-0.52291±j7.6698	1.2207	0.0680	$\omega_{23} = 29.1\%$ $\delta_{23} = 29.1\%$	$e_{d23} = 5.11\%$
(12)	$\lambda_{147}, \lambda_{148}$	-0.65283±j7.7293	1.2302	0.0841	$\omega_{27} = 19.2\%$ $\delta_{27} = 18.9\%$	$e_{d27} = 4.13\%$
(13)	$\lambda_{145}, \lambda_{146}$	-0.78718±j8.2034	1.3056	0.0955	$e_{d20} = 25.9\%$ $e_{q20} = 23.1\%$	$e_{q20} = 2.1\%$
(14)	$\lambda_{143}, \lambda_{144}$	-0.8635±j8.9488	1.4242	0.0961	$\omega_{13} = 25.5\%$ $\delta_{13} = 25.5\%$	$e_{q13} = 7.18\%$
(15)	$\lambda_{141}, \lambda_{142}$	-0.9024±j10.1986	1.6232	0.0881	$e_{d13} = 29.6\%$ $e_{q13} = 24.8\%$	$e_{q13} = 9.7\%$

Since the test system consists of five areas, there are many problems related to interarea modes. The problem is because of weak tie-line connection between them. To highlight the mode shades of the test system, the lowest damping modes of the test system with Model 2 as well as Model 3 are discussed in the following section.

C. Mode Shades of Test System

The interarea modes are named so because in these modes, the participating machines divide into two groups, and the two groups oscillate against each other. If the interarea modes are poorly damped, or unstable, then the two groups may lose synchronism completely and this leads to system breakdown. The phenomenon of all the machines dividing into two groups may be better understood by the help of mode shapes. Mode shapes are the polar plots of the eigenvectors of a mode corresponding to the desired states.

Modes shapes, or the right eigenvectors, give an insight into the relative activity of state variables in each mode. They are obtained from the right eigenvectors, v_i , in the following equation.

$$Av_i^r = \lambda_i v_i^r \quad (13)$$

The larger the magnitude of the element in v_i^r , the more observable of that state variable is. In this research, the state variable, generator speed (ω_i), is used for analysis. Mode shape plots of generator speed of the corresponding case studies in Table I are illustrated in Figs. 11 and 12, respectively. In all the cases, the two groups of machines oscillating against each other can easily be observed. The division of machines into opposing groups is evident in both the cases. In all figures above, the two largest magnitudes of the mode shape elements represents the generator speed: ω_{14} and ω_2 .

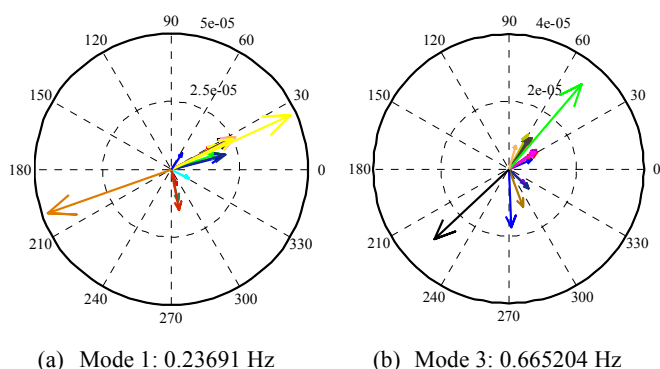


Fig. 11 Mode shapes of test system implementing Model 2

These two larger magnitudes are pointing out the most observable state variables. In can be observed that ω_{14} is the most observable in Mode 1 of both models whereas ω_8 is the most observable in Mode 3 of first case and ω_2 for the later. These observations will later be useful in input signal selection for damping control design.

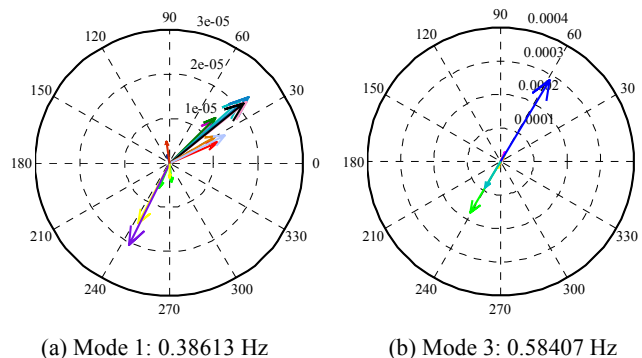


Fig. 12 Mode shapes of test system implementing Model 3

V. CONCLUSION AND FUTURE WORK

This paper presents the Myanmar national grid model for small signal stability analysis being its implementation in a free and open source software; namely, Power System Analysis Toolbox (PSAT). The model takes into account detailed modeling in the assessment of the system's behavior. Dynamic modeling of test system, MEPE power system, in PSAT has been described using detailed dynamic models and newly developed models (especially typical hydro turbine and governor model, Model 3) because more than three quarters of the MEPE grid electric generating stations are hydro power plants. Well-established linear-algebra analysis method, eigenvalue analysis, has been employed to determine the small signal dynamic behavior of test system. Linearized model of test system has been studied by analyzing four properties: eigenvalues, frequencies of oscillation, damping ratios and mode shapes.

The values of parameters in hydro turbine and governor models can impact system oscillations. According to results, the system oscillations cannot be totally fixed by hydro turbine and governor control, but can be improved in some degree through parameter tuning. This study didn't include the PSSs installed at the generating stations. According to results, the MEPE test system is a poor damping system and needs to be stabilized. In order to damp out of low frequency oscillations and to improve power system stability, installing an appropriate number of control devices at appropriate locations within the power system is required. Therefore, to evaluate and observe the optimal location for installing power system oscillation dampers such as PSSs will be the consecutive research.

ACKNOWLEDGMENT

The author would like to thank to his teachers and colleagues from MTU for their support and understanding during this research. The author greatly expresses sincere thanks to all persons whom will concern to support in preparing this research article and for their technical feedback on important issues. The author wishes to express sincere appreciation to the faculty and staffs of MEPE for providing the required data and information.

REFERENCES

- [1] Dysko A, Leithead WE, O'Reilly J., "Enhanced power system stability by coordinated PSS design," IEEE Transl. Power Syst, vol. 25, 2010, pp.413-422.
- [2] Johansson N., Angquist L, Nee H., "An adaptive controller for power system stability improvement and power flow control by means of a thyristor switched series capacitor (TCSC)," IEEE Tansl. Power Syst, vol. 25, 2010, pp. 381-391.
- [3] Ayres HM, Kopcak I, Castro MS, Milano F, da Costa VF, "A didcate procedure for designing power oscillation dampers of FACTS devices," Simul. Model Practice Theory, vol. 18, 2010, pp. 896-909.
- [4] Khodabakhshian A, Hemmati R., "Robust decentralized multi-machine power system stabilizer design using quantitative feedback theory," Electric Power Energy Syst., vol. 41, 2010, pp. 112-119.
- [5] Radaideh SM, Dejdawi IM, Mushtaha MH, "Design of power system stabilizers using two level fuzzy and adaptive neuro-fuzzy interface systems," Electric Power Energy Syst., vol. 35, 2010, pp. 47-56.
- [6] Haussan LH, Moghavvemi M, Almurib HAF, Muttaqi KM, Du H, "Damping of low frequency oscillations and improving power system stability via auto-tuned PI stabilizer using Takagi-Sugeno fuzzy logic," Electric Power Syst., vol. 58, 2012, pp. 72-85.
- [7] Hujan X, Haozhong Ch, Haiyu L., "Optimal reactive power flow incorporating static voltage stability based on multi-objective adaptive immune algorithm," Energy Convers. Manage., vol. 49, 2008, pp. 1175-1181.
- [8] Kundur P, *Power System Stability and Control*, New York, USA, McGraw-Hill, 1994.
- [9] Anderson PM, Fouad AA, *Power System Control and Stability*, 2nd Edn., Manhattan, USA, John Wiley & Sons, 2003.
- [10] Bikash P, Balarko C, *Robust Control in Power System*, New York, USA, Springer Science & Business Media, 2005.
- [11] Wilkinson J, *The Algebraic Eigenvalue Problem*, Oxford University Press, 2004.
- [12] Carlos E., Ugalde-Loo, Enrique Acha, Eduardo Liceaga-Castro, "Multi-machine power system state space modeling for small signal stability assessments," Applied Math. Modelling, vol. 37, 2013, pp. 10141-10161.
- [13] Myint Aung, "Present and future power sector development in Myanmar," MEPE, Nay Pyi Taw, 2012.
- [14] Wei Li, Luigi Vanfretti, Yuwa Chompoobutrgool, "Development and implementation of hydro turbine and governor models in a free and open source software package," Simul. Model. Practice, vol. 24, 2012, pp. 84-102.
- [15] Jan Machowski et al., *Power Systems Dynamics (Stability and Control)*, 2nd Edn, Wiley & Sons Publication, 2008.
- [16] Federico Milano, "An open source power system analysis toolbox," IEEE Trans Power Syst, vol. 20 (3), August 2005, pp. 1199-1206.
- [17] Federico Milano, *Documentation for Power System Analysis Toolbox*, 2010.
- [18] Ghosh Sudipa, Senroy Nilanjan, "The localness of electromechanical oscillations in power systems," Int J. Elect. Power Energy Syst., vol. 42, 2012, pp. 306-313.
- [19] Fernandez RD, Mantz RI, Battaiotto PE, "Impact of wind farms on a power system: an eigenvalue analysis approach," Renew Energy, vol. 32 (10), 2007, pp. 1676-1688.
- [20] Kyaw Swar Soe Naing, "Fuel mix requirements for power generation in Myanmar," MEPE, Nay Pyi Taw, 2013.
- [21] ADB, *Energy Sector Initial Assessment Myanmar*, 2013.